

# Submicrosecond Surface-Induced Dissociation of Peptide Ions in a MALDI TOF MS

Chaminda M. Gamage, Facundo M. Fernández,<sup>†,‡</sup> Krishnamoorthy Kuppannan,<sup>†,§</sup> and Vicki H. Wysocki\*

Department of Chemistry, University of Arizona, Tucson, Arizona 85721

**Surface-induced dissociation (SID) has been implemented in a matrix-assisted laser desorption/ionization time-of-flight mass spectrometer (MALDI TOF MS), allowing production of tandem mass spectrometric information for peptide ions (MALDI TOF SID TOF). The instrument retains the standard operational modes such as the reflectron monitoring of the MALDI-generated intact ions and postsource decay. We show through ion trajectory simulations and experimental results that implementing SID in a commercial MALDI TOF spectrometer is feasible and that the SID products in this instrument fall in an observation time frame that allows the specific detection of fast-fragmentation channels. The instrument design, pulse timing sequence, and high-voltage electronics together with SID spectra of MALDI-generated peptide ions are presented. Standard peptides such as YGGFLR, angiotensin III, fibrinopeptide A, and des-Arg<sup>1</sup>-bradykinin were dissociated by means of hyperthermal collisions with a gold surface coated with a self-assembled monolayer of 2-(perfluorodecyl)ethanethiol. With the extraction fields and the short observation times used, the spectra obtained show intense low-mass ion signals such as immo-nium, b<sub>2</sub>, b<sub>3</sub>, and y<sub>2</sub> ions. TOF data analysis involved matching simulated and experimental flight times and indicates that the observed fragments are produced at ~250 ns after the precursor ion collides with the surface. This submicrosecond gas-phase fragmentation time frame is complementary to the observation time frame of existing SID spectrometers, which are on the order of 10 μs for tandem quadrupoles and are larger than a few milliseconds for SID implemented in Fourier transform ion cyclotron resonance spectrometers.**

Matrix-assisted laser desorption/ionization (MALDI)<sup>1,2</sup> is a highly sensitive ionization technique that allows for the formation of intact gas-phase molecular ions of peptides, proteins, and other

biomolecules. In typical MALDI experiments, a pulsed UV laser beam is focused onto a sample that is cocrystallized with an acidic “matrix” compound. The matrix molecules absorb the laser radiation assisting in the desorption and ionization of the analyte.<sup>3,4</sup> Subfemtomolar detection limits have been reported for peptides using MALDI.<sup>5</sup> MALDI primarily produces singly charged ions<sup>6</sup> making peptide spectral interpretation straightforward in comparison to ionization methods such as electrospray ionization<sup>7</sup> that produce multiply charged ions. MALDI couples naturally to time-of-flight (TOF) mass analyzers because the pulsed nature of the ion production event matches the start–stop operation of TOF analyzers.<sup>8</sup> MALDI TOF MS takes advantage of both the high sensitivity of MALDI and the unique features of TOF such as a large mass range (theoretically unlimited), high throughput, and fast (nonscanning) acquisition of the mass spectrum. The mass resolution achieved by early MALDI TOF spectrometers was highly affected by the initial kinetic energy and spatial spread of the MALDI-generated ions.<sup>9</sup> High-resolution MALDI analysis was not feasible until delayed ion extraction was used to compensate for the spatial spread of the ions produced at the source.<sup>10</sup> The use of an ion mirror (reflectron-TOF) further improved the mass resolution by compensating for the kinetic energy spread of the ions.<sup>9</sup> After attaining high spectral resolution (10 000 or more at fwhm), MALDI TOF MS became an invaluable analytical method used successfully in protein sequencing schemes such as the “peptide mass fingerprinting” approach first described by Stults and co-workers.<sup>11</sup>

Most protein identification methods require obtaining structural information from gas-phase peptide fragmentation reactions, and as such, they rely on tandem mass spectrometry.<sup>12</sup> Although MALDI TOF is an excellent method for obtaining molecular weight information from unknown molecules, production of the tandem mass spectrometric (MS/MS) information needed for

\* Corresponding author. Phone: (520) 621 2628. Fax: (520) 621 8407. E-mail: vwysocki@email.arizona.edu.

<sup>†</sup> Present address: School of Chemistry and Biochemistry, Georgia Institute of Technology, 770 State St., Atlanta, GA 30332-0400.

<sup>‡</sup> Authors contributed equally.

<sup>§</sup> Present address: College of Pharmacy, University of Arizona, Room 205, 1703 E. Mabel St. Tucson, AZ 85721.

(1) Karas, M.; Bachmann, D.; Bahr, U.; Hillenkamp, F. *Int. J. Mass Spectrom. Ion Processes* **1987**, *78*, 53–68.

(2) Hillenkamp, F.; Karas, M. *Int. J. Mass Spectrom.* **2000**, *200*, 71–77.

(3) Knochenmuss, R.; Zenobi, R. *Chem. Rev.* **2003**, *103*, 441–452.

(4) Knochenmuss, R. *Anal. Chem.* **2003**, *75*, 2199–2207.

(5) McLean, J. A.; Russell, D. H. *J. Proteome Res.* **2003**, *2*, 427–430.

(6) Karas, M.; Gluckmann, M.; Schafer, J. *J. Mass Spectrom* **2000**, *35*, 1–12.

(7) Fenn, J. B.; Mann, M.; Meng, C. K.; Wong, S. F.; Whitehouse, C. M. *Science* **1989**, *246*, 64–71.

(8) Muddiman, D. C.; Bakhtiar, R.; Hofstadler, S. A.; Smith, R. D. *J. Chem. Educ.* **1997**, *74*, 1288–1292.

(9) Cotter, R. J. *Anal. Chem.* **1999**, *71*, 445A–451A.

(10) Wiley, W. C.; McLaren, I. H. *Rev. Sci. Instrum.* **1955**, *26*, 1150–1157.

(11) Henzel, W. J.; Billeci, T. M.; Stults, J. T.; Wong, S. C.; Grimley, C.; Watanabe, C. *Proc. Natl. Acad. Sci. U.S.A.* **1993**, *90*, 5011–5015.

(12) Dongre, A. R.; Eng, J. K.; Yates, J. R., III. *Trends Biotechnol.* **1997**, *15*, 418–425.

further structural investigation of the precursor ions is complicated by the pulsed nature of MALDI. The standard MALDI TOF mass spectrometer relies on postsource decay (PSD) for structural elucidation. During PSD, unimolecular decay of laser-excited ions in the field-free region of the TOF mass analyzer is used to produce MS/MS data.<sup>13–16</sup> Unfortunately, the reproducibility and extent of the internal energy deposition during MALDI PSD are based on the peptide and matrix identity as well as the laser fluence and the in-plume collisions, which are not easy to control or monitor.<sup>17</sup> Another difficulty of PSD is the complex acquisition and calibration procedures needed with linear ion mirrors that are scanned as “kinetic energy filters” during sample analysis. Only MALDI TOF mass spectrometers equipped with curved field ion mirrors<sup>18</sup> are able to record PSD spectra without stepping the reflectron voltage. However, even with a curved field reflectron, PSD still relies on the abundance of metastable ions produced by excess energy from laser and in-plume collision processes.

Different types of tandem mass spectrometers with MALDI ionization are currently available. High-end ion-trapping mass spectrometers such as Fourier transform ion cyclotron resonance mass spectrometers (FTICR MS) equipped with MALDI sources can produce structural information of the precursor ions by activation via sustained off-resonance irradiation (SORI CID),<sup>19</sup> infrared multiphoton dissociation<sup>20</sup> and electron capture dissociation.<sup>21</sup> More modest trapping mass spectrometers such as quadrupole ion traps (QIT) lack the spectral acquisition speed, mass resolution, and simplicity of TOF mass spectrometers. High-resolution MS/MS can be obtained in MALDI tandem quadrupole-TOF instruments (QTOF), where orthogonal acceleration is used for collisionally cooled ions fragmented in a multipolar ion guide.<sup>22</sup> However, MS/MS capabilities of QTOF instruments can be limited by the mass range of the mass-selection quadrupole and the limited dissociation of large singly charged precursor ions. Recently, high-energy CID in combination with two tandem-in-space TOF mass spectrometers (MALDI TOF/TOF) and a Bradbury–Nielsen-type<sup>23</sup> ion gate system for mass selection has been described.<sup>24</sup> Although appealing due to their high performance, commercial MALDI TOF/TOF mass spectrometers are large and not yet in as widespread use as QIT or QTOF instruments.

Although most commercial MS/MS instruments utilize gas-phase collisions for collisional activation, surface-induced dissociation (SID) is an efficient ion activation method that is a potential candidate for activation in MALDI MS/MS. It has been shown that SID can achieve high kinetic energy to internal energy conversion efficiency and thus it is attractive for fragmenting singly charged ions.<sup>25,26</sup> Several groups have incorporated SID into TOF mass spectrometers. Schey and co-workers first demonstrated the feasibility of SID in TOF analyzers using a stainless steel surface placed between two orthogonal TOF regions.<sup>27</sup> The mass resolution and range of this instrument were further improved by incorporating an electrostatic reflectron at the second TOF stage.<sup>28</sup> This concept was then further pursued by Whetten and co-workers,<sup>29,30</sup> Zare and co-workers,<sup>31,32</sup> and de Maaijer-Gielbert and co-workers<sup>33,34</sup> by implementing SID in a single TOF analyzer with the collision target placed after or between the ring lenses of an ion reflectron. Haney and Reiderer<sup>35</sup> and Wysocki et al.<sup>36</sup> continued to improve the resolution of these setups by incorporating a voltage pulse to achieve delayed extraction of SID ions at the surface. In recent work, Russell and co-workers fragmented peptide ions produced by MALDI by using SID after a first separation step in an ion mobility drift tube operated at reduced pressure.<sup>37,38</sup> Jungclas et al. have demonstrated grazing-incidence SID of peptide ions produced by MALDI.<sup>39</sup> In a recent paper, Laskin et al. reported an intermediate-pressure MALDI source interfaced to a 6-T FTICR MS equipped for surface-induced dissociation. They showed that FTICR SID produced better peptide sequence coverage than SORI CID.<sup>40</sup>

In this paper, we show the feasibility of performing MALDI TOF SID of peptide ions using near-normal collision geometry in a benchtop instrument. MALDI TOF SID is achieved by replacing the drift tube normally used in linear operation mode with a movable surface assembly placed immediately after the reflectron, without affecting the standard single-stage MS monitoring mode. Delayed extraction using high-voltage pulsing electronics is

- (13) Spengler, B.; Kirsch, D.; Kaufmann, R. *Rapid Commun. Mass Spectrom.* **1991**, *5*, 198–202.
- (14) Spengler, B.; Kirsch, D.; Kaufmann, R.; Jaeger, E. *Rapid Commun. Mass Spectrom.* **1992**, *6*, 105–108.
- (15) Spengler, B. *J. Mass Spectrom.* **1997**, *32*, 1019–1036.
- (16) Chaurand, P.; Luetzenkirchen, F.; Spengler, B. *J. Am. Soc. Mass Spectrom.* **1999**, *10*, 91–103.
- (17) Zenobi, R.; Knochenmuss, R. *Mass Spectrom. Rev.* **1998**, *17*, 337–366.
- (18) Cordero, M. M.; Cornish, T. J.; Cotter, R. J.; Lys, I. A. *Rapid Commun. Mass Spectrom.* **1995**, *9*, 1356–1361.
- (19) Shukla, A. K.; Futrell, J. H. *Mass Spectrom. Rev.* **1993**, *12*, 211–255.
- (20) Little, D. P.; Speir, J. P.; Senko, M. W.; O'Connor, P. B.; McLafferty, F. W. *Anal. Chem.* **1994**, *66*, 2809–2815.
- (21) Zubarev, R. A.; Horn, D. M.; Fridriksson, E. K.; Kelleher, N. L.; Kruger, N. A.; Lewis, M. A.; Carpenter, B. K.; McLafferty, F. W. *Anal. Chem.* **2000**, *72*, 563–573.
- (22) Loboda, A. V.; Krutchinsky, A. N.; Bromirski, M.; Ens, W.; Standing, K. G. *Rapid Commun. Mass Spectrom.* **2000**, *14*, 1047–1057.
- (23) Kimmel, J. R.; Engelke, F.; Zare, R. N. *Rev. Sci. Instrum.* **2001**, *72*, 4354–4357.
- (24) Medzhradzky, K. F.; Campbell, J. M.; Baldwin, M. A.; Falick, A. M.; Juhasz, P.; Vestal, M. L.; Burlingame, A. L. *Anal. Chem.* **2000**, *72*, 552–558.

- (25) Laskin, J.; Denisov, E.; Futrell, J. J. *Phys. Chem. B* **2001**, *105*, 1895–1900.
- (26) Grill, V.; Shen, J.; Evans, C.; Cooks, R. G. *Rev. Sci. Instrum.* **2001**, *72*, 3149–3179.
- (27) Schey, K.; Cooks, R. G.; Grix, R.; Wollnik, H. *Int. J. Mass Spectrom. Ion Processes* **1987**, *77*, 49–61.
- (28) Schey, K. L.; Cooks, R. G.; Kraft, A.; Grix, R.; Wollnik, H. *Int. J. Mass Spectrom. Ion Processes* **1989**, *94*, 1–14.
- (29) Beck, R. D.; St. John, P.; Homer, M. L.; Whetten, R. L. *Science* **1991**, *253*, 879–883.
- (30) Yeretzian, C.; Beck, R. D.; Whetten, R. L. *Int. J. Mass Spectrom. Ion Processes* **1994**, *135*, 79–118.
- (31) Williams, E. R.; Jones, G. C., Jr.; Fang, L.; Zare, R. N.; Garrison, B. J.; Brenner, D. W. *J. Am. Chem. Soc.* **1992**, *114*, 3207–3210.
- (32) Williams, E. R.; Fang, L.; Zare, R. N. *Int. J. Mass Spectrom. Ion Processes* **1993**, *123*, 233–241.
- (33) de Maaijer-Gielbert, J.; Beijersbergen, J. H. M.; Kistemaker, P. G.; Weeding, T. L. *Int. J. Mass Spectrom. Ion Processes* **1996**, *153*, 119–128.
- (34) de Maaijer-Gielbert, J.; Somogyi, A.; Wysocki, V. H.; Kistemaker, P. G.; Weeding, T. L. *Int. J. Mass Spectrom. Ion Processes* **1998**, *174*, 81–94.
- (35) Haney, L. L.; Riederer, D. E. *Anal. Chim. Acta* **1999**, *397*, 225–233.
- (36) Nikolaev, E. N.; Somogyi, A.; Smith, D. L.; Gu, C.; Wysocki, V. H.; Martin, C. D.; Samuelson, G. L. *Int. J. Mass Spectrom.* **2001**, *212*, 535–551.
- (37) Stone, E. G.; Gillig, K. J.; Ruotolo, B. T.; Russell, D. H. *Int. J. Mass Spectrom.* **2001**, *212*, 519–533.
- (38) Stone, E.; Gillig, K. J.; Ruotolo, B.; Fuhrer, K.; Gonin, M.; Schultz, A.; Russell, D. H. *Anal. Chem.* **2001**, *73*, 2233–2238.
- (39) Wieghaus, A.; Schmidt, L.; Popova, A. M.; Komarov, V. V.; Jungclas, H. *Rapid Commun. Mass Spectrom.* **2000**, *14*, 1654–1661.
- (40) Laskin, J.; Beck, K. M.; Hache, J. J.; Futrell, J. H. *Anal. Chem.* **2004**, *76*, 351–356.

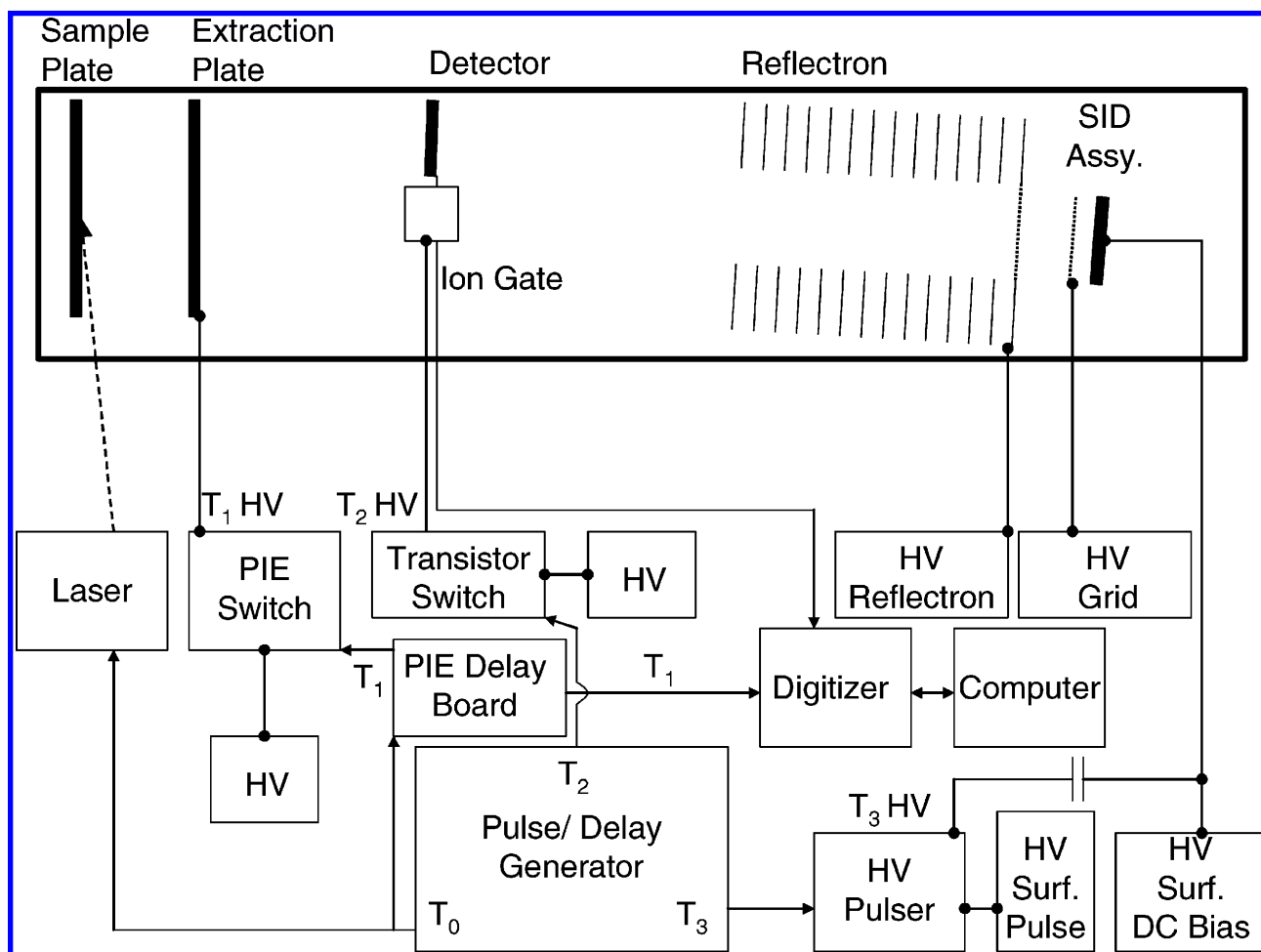


Figure 1. Block diagram of the power supplies and triggering hardware. The pulse/delay generator is used to trigger the  $N_2$  laser. The same TTL pulse is used to trigger the extraction delay generator board that enables the pulsed ion extraction switch (PIE) after a delay of 235 ns. The matrix blanking ion gate and the surface pulse are also triggered by the delay generator to ensure reproducibility between laser shots. The MCP detector ( $-1750$  V) records the ion counts that are digitized at 1 GHz.

employed at the surface to extract the SID ions. Using the extraction geometry described here and the extraction voltages that we have applied to date, the SID spectra are dominated by low-mass fragments such as immonium ions,  $b_2$ ,  $b_3$ , and  $y_2$  ions. As in any MS/MS experiment, the observed fragments in a given spectrum are determined in part by the observation time window of the mass spectrometer used. The observation time frame for the instrument described here allows the detection of fragments resulting from very fast fragmentation channels. Laskin et al. have shown that the observation of higher mass peptide fragments resulting from slow-fragmentation pathways requires observation times on the order of milliseconds. Conversely, they also proposed that some fragments are formed in a very short time frame and have suggested a "shattering"-type fragmentation mechanism.<sup>41</sup>

In this MALDI TOF SID work, SID data for several peptides are presented to illustrate the influence of collision/collection angle, surface extraction delay, and collision energy on the appearance of the spectra. The effect of the surface voltage pulse delay on mass resolution is presented and compared to SIMION models. A procedure to estimate the fragmentation time frame based on matching the experimental flight time of fragment ions

to time-of flight values determined by ion trajectory simulations is also described. The knowledge obtained from these experiments contributes to the understanding of ion fragmentation kinetics including an assessment of whether "shattering" products are detected and to improvements in the design of future TOF-SID spectrometers.

## EXPERIMENTAL SECTION

**Instrumentation.** A benchtop MALDI TOF MS (Proflex, Bruker Daltonics) was converted to SID operation by removing the drift tube found immediately after the reflectron (used in linear mode of operation) and introducing a flange-mounted surface assembly instead (Figure 1). No machining of the drift chamber or modification of any of the remaining hardware was required. The surface assembly (Figure 2) consists of a collision target retained by a brass plate, followed by an extraction grid mounted on a second brass holder. This Ni grid (20-line mesh, BMC Industries Inc., St Paul, MN) was attached to the brass holder using copper adhesive tape (Part No. 3M 1181, 3M, Maplewood, MN). The grid holder and the surface holder were electrically isolated from each other by a 5-mm-thick Macor spacer. A 20 by 20 mm square opening with smoothed corners was machined, in the center of both the brass surface holder and the Macor spacer, exposing the collision target. The extraction grid, brass holders,

(41) Laskin, J.; Bailey, T. H.; Futrell, J. H. *J. Am. Chem. Soc.* **2003**, *125*, 1625–1632.

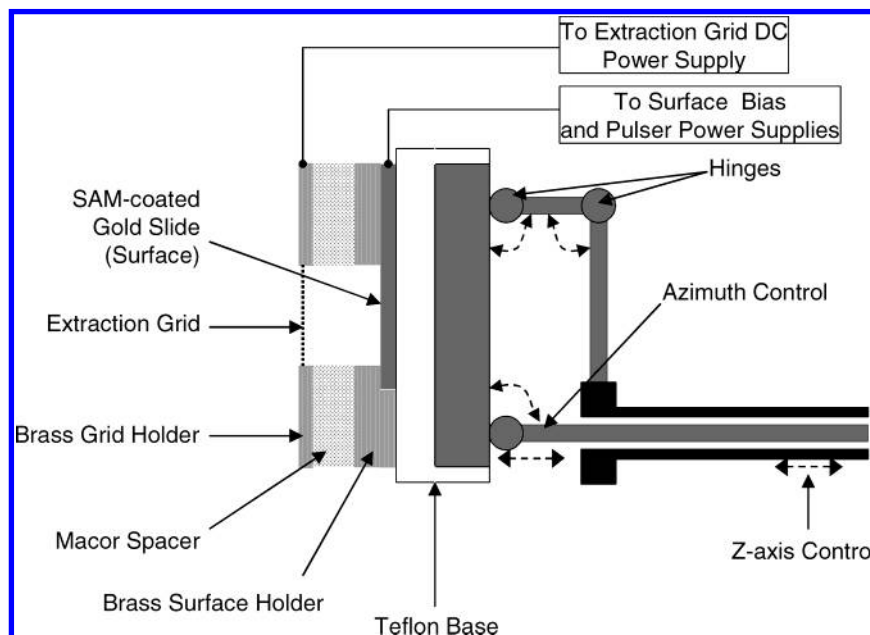


Figure 2. Schematic of the surface assembly placed at the back end of the reflectron. The circles represent hinges that allow changing the azimuthal angle. The surface assembly is held in position by two independent, concentric arms. When the inner arm is moved in the z-axis direction, the outer (cylindrical) arm remains in place, and thus, the assembly rotates at the hinges changing the surface azimuthal angle. The outer arm is moved if the surface assembly position is to be changed as a whole with respect to the reflectron. Figure not to scale; extraction grid and exposed SAM surface are  $20 \times 20 \text{ mm}^2$  squares, brass grid holder outer diameter of  $\sim 50 \text{ mm}$  with a thickness of  $\sim 1 \text{ mm}$ , Macor spacer thickness  $\sim 5 \text{ mm}$ ; brass surface holder thickness  $\sim 2.5 \text{ mm}$ .

Macor spacer, and collision target were mounted on a custom-built assembly consisting of a z-movable stage (model BLM-275-1, MDC, Hayward, CA) combined with a set of hinges, allowing variation of the angle between the target surface and the plane parallel to the last reflectron electrode (Figure 2). The minimum increment in azimuthal angle allowed by this setup was  $0.5^\circ$ . The z-stage used to change the azimuthal angle was mounted on a second (independent) z-stage (Part No. KZLSM275010, Kurt J. Lesker, Clairton, PA) that was used to vary the distance between the surface assembly and the reflectron back plate.

Direct current bias voltages for the extraction grid and the collision surface were supplied by rack-mounted high-voltage power supplies (EH Series, Glassman, High Bridge, NJ). The timing of the surface high-voltage delayed-extraction pulse, the laser pulse, and the voltage pulse applied to the matrix blanking electrode was provided by TTL signals generated with a digital delay/pulse generator (model PDG-2510, Directed Energy Inc., Fort Collins, CO). The surface extraction pulse was provided by a high-voltage pulser (model PVX-4140, Directed Energy Inc.). This pulser was connected to a Glassman high-voltage dc power supply to define the pulse amplitude. The pulsed and static voltages applied to the surface are coupled capacitively using a  $920 \text{ pF}$   $40\text{-kV}$  capacitor. All the voltages applied to the surface and extraction grid were determined by measuring the monitor outputs of the Glassman power supplies with a four-digit digital multimeter (model 187, Fluke, Everett, WA). With this monitoring arrangement, the high voltages used during the experiments ( $10\text{--}17 \text{ kV}$ ) could be controlled with a precision of  $\pm 5 \text{ V}$ .

**Materials and Samples.** Glass surfaces coated with a  $50\text{-\AA}$  layer of titanium followed by a  $1000\text{-\AA}$  layer of gold (Evaporated Metal Films Corp., Ithaca, NY) were used as substrates for preparing the SID collision targets. The Au-coated slide was UV

cleaned for 30 min, rinsed with ethanol, and immersed in a  $1 \text{ mM}$  ethanolic solution of 2-(perfluorodecyl)ethanethiol for 12 h. After this, the surface was immersed in pure ethanol and cleaned in an ultrasonic bath for 5 min. Sonication was repeated two times using fresh ethanol volumes. Finally, the surface was air-dried and introduced into the instrument, which was pumped overnight down to  $1.2 \times 10^{-7} \text{ Torr}$ . The thiol used for self-assembled monolayer (SAM) formation on the SID collision target (2-(perfluorodecyl)ethanethiol) was synthesized by the Chemical Synthesis Facility of the Department of Chemistry, University of Arizona. In future experiments, diamond thin films, which have been used previously in SID experiments,<sup>40</sup> will be evaluated as surface targets for this instrument.

The matrix used for MALDI,  $\alpha$ -cyano-4-hydroxycinnamic acid (CHCA), was purchased from Aldrich Chemical Co. Inc (St. Louis, MO) and used without further purification. A matrix solution was prepared by saturating CHCA in a 7:3:0.1 v/v/v mixture of deionized water, acetonitrile (Sigma), and trifluoroacetic acid (Sigma). All the peptides used throughout this work were purchased from Sigma and used without any further purification. Peptide stock solutions ( $100 \mu\text{M}$ ) were prepared in deionized water (Milli-Q Plus System, Millipore, Billerica, MA) with 0.1% trifluoroacetic acid added. Peptide solutions were kept refrigerated for a maximum of two weeks, after which they were discarded. Prior to analysis,  $1 \mu\text{L}$  of the peptide solution was mixed with  $9 \mu\text{L}$  of a saturated CHCA solution. One microliter of this analyte–matrix solution was spotted and air-dried on the stainless steel target surface of the MALDI spectrometer. A  $337\text{-nm}$  nitrogen laser with an average energy of  $150 \mu\text{J/pulse}$  was used for ionization (model VSL337i, Laser Science, Inc.).

The observed signals in the SID spectra were matched to the expected  $m/z$  values obtained from the MS-Product routine in

ProteinProspector v 4.0 (<http://prospector.ucsf.edu>). The peptide fragment ion nomenclature used here is the one suggested by Roepstorff and Fohlman<sup>42</sup> and later modified by Biemann.<sup>43</sup> A two-point calibration procedure included in Bruker's XMASS 5.0 software was used for spectral calibration purposes and required assignment of  $m/z$  values of two fragment ions. The calibrated spectra were smoothed by adjacent averaging and baseline-corrected with Origin 6.0 (OriginLab, Natick, MA). Ion trajectory simulations were performed on a 3.06-GHz Intel Pentium IV processor-PC using SIMION v. 7.0 (Idaho National Engineering and Environmental Laboratory, Idaho Falls, ID).

## RESULTS AND DISCUSSION

**Modification of a Commercial MALDI TOF Spectrometer for SID Operation.** Figure 1 shows the experimental setup used to study surface-induced dissociation of protonated oligopeptide ions produced by MALDI. Our objective was to develop an SID design that could be later implemented by other MALDI users in their own spectrometers without major modifications or cost. Simplicity and ruggedness were the main characteristics sought in the design. As mentioned in the Experimental Section, our surface assembly has features that enable the user to vary the distance between the extraction grid and the last reflectron lens and change the angle inscribed by the source, the surface, and the detector (azimuthal angle) (Figure 2). These features of the SID assembly are only necessary to enable full optimization of our first prototype, but should not be needed in future simplified versions of the setup described here.

Limited tandem TOF capabilities<sup>44</sup> were added to the instrument by reconfiguring the matrix-blanking high-voltage electronics. In the original configuration provided by the vendor, the ion gate (Figure 1) works as a low-mass filter device. Ions with time of flight shorter than the time set via software, usually the matrix ions, are deflected. After this set time is reached, the electrode is grounded and all ions are transmitted. In preparation for experiments with peptide mixtures, the ion gate transistor switch was reconfigured to provide a coarse mass selection of the precursor ion. This selection is achieved by pulsing the ion gate to ground for a 1–1.5- $\mu$ s window centered at the desired TOF. Due to the fringing fields projected by this electrode geometry, a mass selection interval of only 50 mass units was achieved. Better mass selection could be potentially achieved with a Bradbury–Nielsen-type ion gate, where the fringing fields in the direction of the flight trajectory are partially canceled by the alternating polarity of the different wire sets.<sup>23</sup>

The dc voltages applied to the electrostatic optic elements of the spectrometer (Figure 1) for SID operation differ from the ones used in normal MALDI TOF reflectron mode. Standard source voltages are generally 19.5 kV for the sample plate and 15.75 kV for the extraction plate. However, for optimal SID fragment mass resolution, the parent ions should be space-focused at the collision surface. The position of the space focus is a function of the ratio of the extraction and acceleration fields.<sup>10</sup> Sensitivity and mass resolution improve at high acceleration voltages, and thus, dc surface voltages at or around 20 kV are desirable. However, it

was not possible to reach this voltage due to intermittent arcing between the surface assembly and the grounded TOF drift chamber. (Modifications are in progress to minimize arcing by replacing brass parts with polished stainless steel.) The sample plate (MALDI target) had to be lowered from 20 kV to a compromise value of 16.2 kV with the extraction plate voltage set to 14.9 kV. The static surface dc bias voltage prior to the surface pulse is set between 200 and 300 V lower than the sample plate to provide collision energies in the hyperthermal energy range (corrected for initial velocity and spatial displacements within the source; see below). The last reflectron plate voltage was decreased with respect to the reflectron mode setting from 16.5 to 5.0 kV. This setting reduces the velocity of the precursor ions by an opposing potential energy gradient in their flight path and partially compensates for the spread in kinetic energies. However, it does not produce a velocity reversal, allowing for the passage of the precursor ions through the reflectron lenses and subsequent collision with the surface. This reflectron setting also reduces the appearance of the metastable PSD ion peaks that interfere with SID ion signals. SID ions were extracted using a surface voltage pulse (capacitively coupled to the surface dc bias) and an extraction grid operated at 12 kV that was placed in front of the collision target resulting in a two-stage extraction of ions formed by surface collision. Initial attempts to perform SID without this extraction grid were unsuccessful although additional recent experiments with a cylindrical surface holder without a grid have resulted in collection of SID products.

A major difference between the present MALDI TOF SID instrument and our previously reported EB/TOF instrument<sup>36</sup> is that, in the latter case, the TOF mass analysis of the scattered ions is performed coaxially, and in the present case, it is done with "V-shaped" optics. However, the instrument concept remains the same. It has been shown that fragment ions produced after surface-induced activation can be scattered at a wide range of angles. For example, the preferential scattering of parent and fragment ions at different angles has been described by Futrell and co-workers<sup>45</sup> and Herman and co-workers<sup>46</sup> for benzene radical cations and their SID fragments. However, scattering of ions from an ion beam impacting at a near-to-normal geometry has not been reported in the literature. For this reason we added the capability of varying the surface azimuthal angle of our surface assembly. Figure 3 shows YGGFLR SID spectra collected at different surface angles. Two results can be pointed out. First, it is clear that there is an angle at which the SID spectrum shows the best overall signal-to-noise ratio (3.75°). The second observation that can be drawn from the results presented in Figure 3 is that at angles smaller than 3° a signal for the protonated parent ion can be seen at  $m/z = 712.8$ . This result is in accordance with the results reported by Jungclas and co-workers, who also used a surface coated with a perfluorinated compound to perform SID.<sup>39</sup> In their work on grazing-incidence SID, they found that, by placing the detector at different positions, different types of ions could be detected. Small fragments corresponding to immonium ions were preferentially detected if the detector was placed closer to the optical axis of the spectrometer, while larger fragments and intact

(42) Roepstorff, P.; Fohlman, J. *Biomed. Mass Spectrom.* **1984**, *11*, 601.

(43) Biemann, K. *Biomed. Environ. Mass Spectrom.* **1988**, *16*, 99–111.

(44) Raska, C. S.; Parker, C. E.; Huang, C.; Han, J.; Glish, G. L.; Pope, M.; Borchers, C. H. *J. Am. Soc. Mass Spectrom.* **2002**, *13*, 1034–1041.

(45) de Clercq, H. L.; Sen, A. D.; Shukla, A. K.; Futrell, J. H. *Int. J. Mass Spectrom.* **2001**, *212*, 491–504.

(46) Worgotter, R.; Kubista, J.; Zabka, J.; Dolejssek, Z.; Mark, T. D.; Herman, Z. *Int. J. Mass Spectrom. Ion Processes* **1998**, *174*, 53–62.

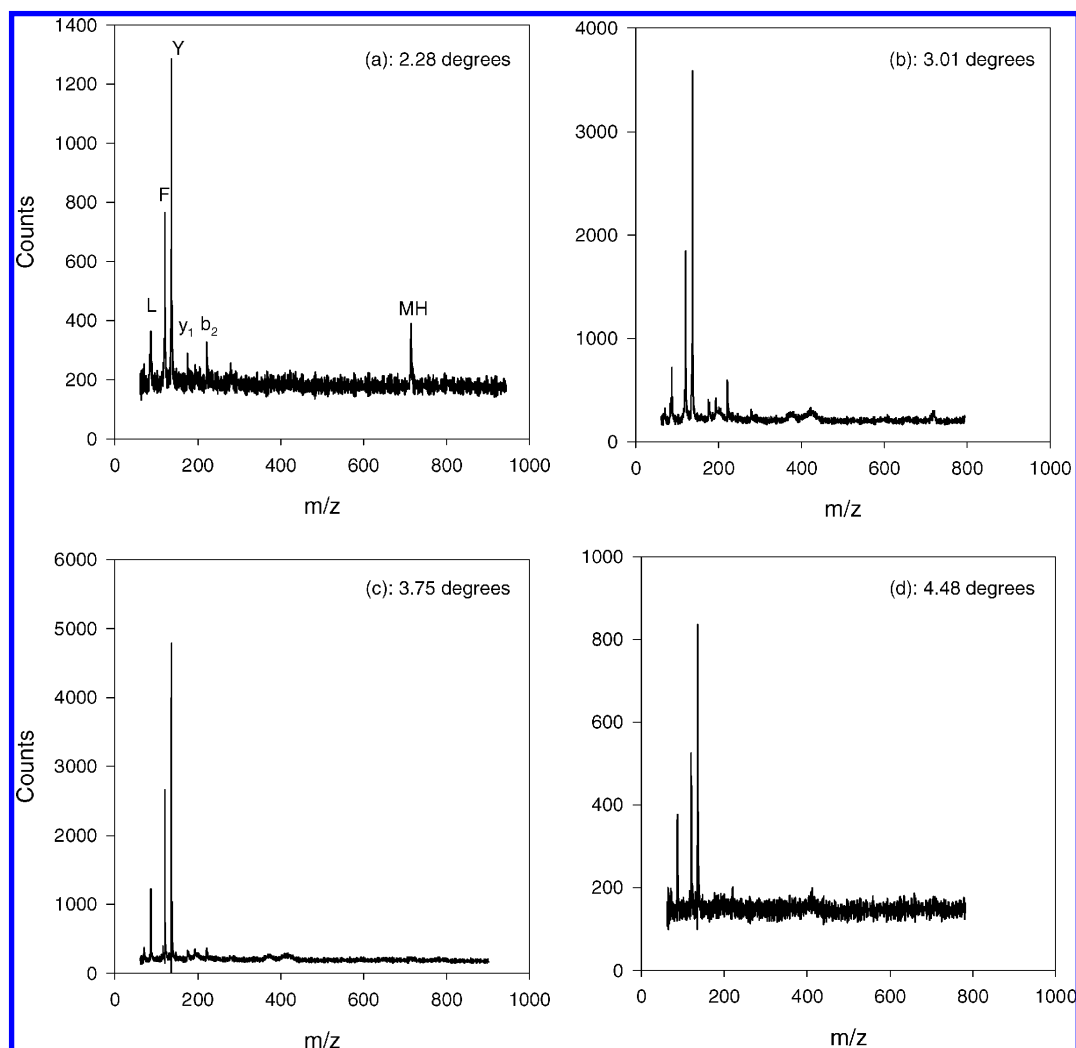


Figure 3. SID spectra of YGGFLR at different azimuthal angles. The azimuthal angle is inscribed in the plane formed by the source, the collision point at the surface, and the MCP detector. An azimuthal angle of zero degrees means that the surface is parallel to the last reflectron plate. The collision surface was rotated as shown in Figure 2.

precursor ions were detected if the signal was monitored at a position farther away from the optical axis of the spectrometer. In practice, a surface angle in the range of 2.5–3.0° was used as a compromise between good sensitivity for the fragment ions and a representative sampling of all the ions formed by SID in this setup. Although the surface angular position was fine-tuned for every peptide studied, no major differences in the optimum azimuthal angle were found.

**System Optimization and Trajectory Simulations Using SIMION 7.0.** Trajectory simulations performed with SIMION 7.0 were used both to understand the behavior of our SID setup and to further optimize it. The initial kinetic energy values needed for SIMION simulations of both analyte and matrix ions (prior to their extraction at the source) were derived from the values for zero accelerating field conditions reported in the literature. Chait et al.<sup>47</sup> reported an average initial velocity for peptide ions produced by MALDI of  $\sim 750 \text{ m s}^{-1}$ . In their study, they also concluded that this initial velocity is not significantly dependent on the analyte mass. Later,<sup>48</sup> they also reported that the initial radial velocity component of MALDI ions is significantly lower

than the axial velocity component thus resulting in a forward peaked ion plume. Russell and co-workers measured larger initial kinetic energies for MALDI-produced ions under nonzero extraction field conditions using an electrostatic analyzer/TOF setup.<sup>49</sup> The kinetic energy values reported by Russell et al. decrease with decreasing extraction field and approximate the values reported by Chait at zero extraction fields. Gluckmann and Karas reported an initial velocity of  $291 \text{ m s}^{-1}$  for the larger insulin ion ( $M_w = 5.8 \text{ kDa}$ ) using CHCA as the MALDI matrix.<sup>50</sup>

In our studies, we used the initial kinetic energy data reported by Chait and co-workers to describe the starting ion population in SIMION. The ions' initial velocities and spatial displacements during the time elapsed before the source extraction plate is pulsed were calculated for a delay of 235 ns (measured experimentally). A total of 20 ions with equal mass to charge but different individual starting coordinates and velocity were input into SIMION. Initial kinetic energies given to the ions spanned the

(48) Zhang, W.; Chait, B. T. *Int. J. Mass Spectrom. Ion Processes* **1997**, *160*, 259–267.

(49) Kinsel, G. R.; Gimmon-Kinsel, M. E.; Gillig, K. J.; Russell, D. H. *J. Mass Spectrom.* **1999**, *34*, 684–690.

(50) Gluckmann, M.; Karas, M. *J. Mass Spectrom.* **1999**, *34*, 467–477.

(47) Beavis, R. C.; Chait, B. T. *Chem. Phys. Lett.* **1991**, *181*, 479–484.

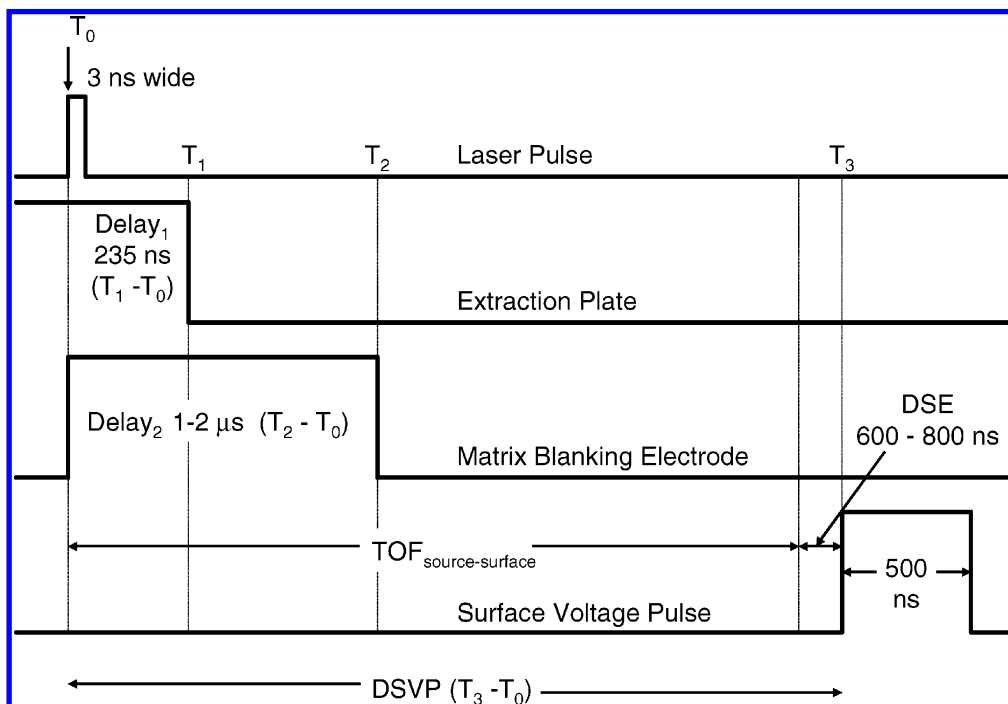


Figure 4. Timing sequence of a single-shot MALDI TOF SID experiment. DSVP, delay of the surface voltage pulse; DSE, delay of the surface extraction.

range of 1.4–5.3 eV, following a Gaussian distribution. The starting angular distribution given to the ions ranged from normal ( $0^\circ$ ) to  $15^\circ$ .<sup>48</sup> Ions were started at the surface of the MALDI sample spot, centered, and incremented over a 1-mm<sup>2</sup> area; no initial position spread in the  $z$ -axis (optical axis) was introduced.

Timing and synchronization of the source and surface extraction pulses are of utmost importance and were included in the simulations via user programs. Figure 4 describes the triggering sequence during system operation. The time elapsed between the laser trigger and the surface impact is directly related to the experimental delay of the surface voltage pulse (DSVP). The experimental DSVP differs only by a few hundred nanoseconds from the surface impact event ( $\text{TOF}_{\text{source-surface}}$ ). This delay is used to improve the mass resolution. During our initial experiments,  $\text{TOF}_{\text{source-surface}}$  values obtained from SIMION simulations were used as the first guess values for the experimental DSVP. After SID data for several peptides were obtained, the experimentally determined DSVP values were plotted against the square root of the mass of the protonated peptide ion in order to obtain the linear plot shown in Figure 5. The experimental DSVP values shown in Figure 5 correspond to a sample plate electrode voltage of 16.2 kV, a source extraction voltage of 14.9 kV, a source lens voltage of 9.8 kV, a reflectron voltage of 5.0 kV, a surface grid voltage of 12.0 kV, and a surface voltage of 15.9 kV. The obtained linear plot ( $r^2 = 0.9988$ ) can be used to further predict experimental DSVP for additional peptides. Figure 5 also shows the simulated  $\text{TOF}_{\text{source-surface}}$  values. The fact that both the simulated and experimental values have similar slopes ( $0.384 \pm 0.002$  and  $0.375 \pm 0.006$ , respectively) is good evidence that our simulations are in agreement with the experiments. The simulated  $\text{TOF}_{\text{source-surface}}$  values are lower than the corresponding experimental DSVP values because in order to obtain optimum resolution for the SID ions we have introduced a small delay between the ions' impact and the surface extraction pulse (Figure 4, "delay of the surface

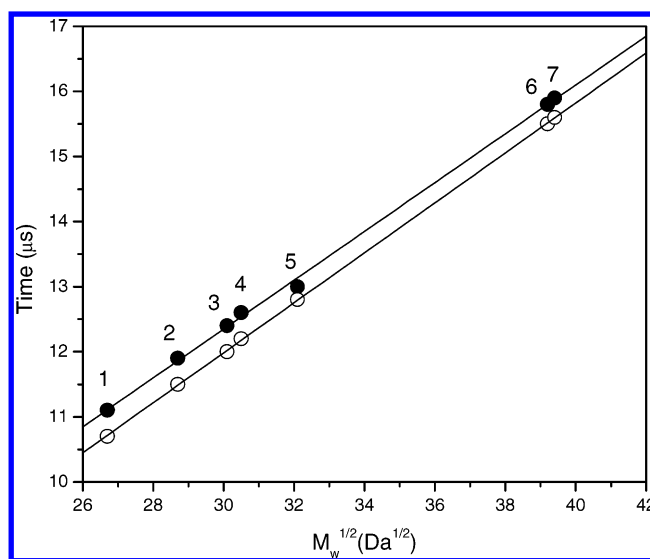


Figure 5. Dependence of the surface voltage pulse delay (time,  $\mu\text{s}$ ) on the square root of the ion's mass. Black symbols: experimental surface pulse delay for SID ion activation (DSVP) corresponding to source-surface time-of-flight plus delay of surface extraction (DSE), White symbols: source-surface time-of-flight simulated with SIMION. 1, YFGGFLR; 2, ASHLGLAR; 3, PPGFSPFR; 4, angiotensin III; 5, LMYPTYLK; 6, fibrinopeptide A; 7, fibrinopeptide B.

extraction", DSE;  $\text{DSVP} = \text{TOF}_{\text{source-surface}} + \text{DSE}$ ). It is well known that, in MALDI, delayed extraction reduces the effect of the ions' spatial and energy spread.<sup>51</sup> During delayed-extraction MALDI, the different broadening mechanisms are allowed to proceed for a given time after which the ion packet is compressed in the flight direction by a pulsed electrical field, reaching a focal point at the detector. However, less attention has been paid to the use

(51) Amft, M.; Moritz, F.; Weickhardt, C.; Grottemeyer, J. *Int. J. Mass Spectrom. Ion Processes* **1997**, *167/168*, 661–674.

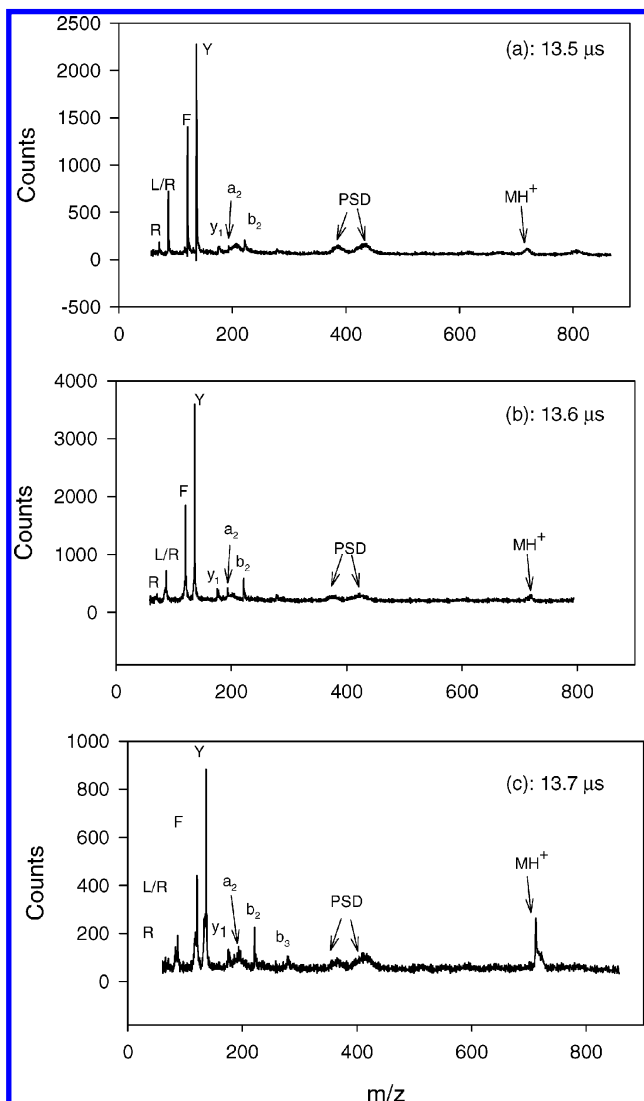


Figure 6. Effect of surface pulse delay (DSVP) on the SID spectra of YGGFLR. Collision energy was 45 eV in each case. A total of 150 shots were collected for each spectrum. PSD peaks were minimized in subsequent experiments (see text).

of delayed extraction as a means of improving the resolution of ions formed at (or near) a collision target during SID. Wysocki and co-workers have reported that the best mass resolution during SID in a coaxial TOF was obtained with a DSE value of a few hundred nanoseconds<sup>36</sup> for a surface extraction field of  $500 \text{ V cm}^{-1}$ .

Figure 6 shows the effect of different surface pulse delays on the mass resolution obtained for SID of YGGFLR protonated ions. The optimum DSVP observed for YGGFLR was  $13.6 \mu\text{s}$  as shown in the spectrum presented in Figure 6b. A DSVP of  $13.5 \mu\text{s}$  resulted in better focusing for the immonium ions (Figure 6a) while a DSVP of  $13.7 \mu\text{s}$  focused larger mass fragments better than the immonium ions (Figure 6c). These results are in agreement with the simulations performed by Franzen,<sup>52</sup> who showed that the commonly used delayed extraction method only focuses ions in a limited mass-to-charge window. Note the additional appearance of unresolved broad signals due to metastable decay of precursor ions. These metastable ion signals were

minimized in subsequent experiments by decreasing the reflectron voltage from 10 (used for spectra shown in Figure 6) to 5.0 kV to defocus the PSD ions (see Figure 8a).

Unlike previous TOF SID experiments utilizing continuous ion extraction at the source<sup>36</sup> where the collision energy was calculated as the source–surface potential difference, the laboratory frame collision energy in MALDI TOF SID is a function of the voltage applied to the sample plate electrode, the voltage applied to the source extraction plate, the time delay employed in the extraction of MALDI ions, and the surface dc voltage bias. Therefore, the collision energies of the peptide ions had to be obtained by simulations rather than by simply subtracting the surface dc voltage bias from that of the sample plate electrode. The “corrected” collision energy can be determined using a plot of the simulated laboratory collision energy versus the source–surface potential difference. Such a plot was obtained for a sample plate voltage of 16.2 kV, an extraction voltage of 14.9 kV, and a 235-ns extraction delay (data not shown). The obtained plot was linear with  $r^2 = 1.00$  and a  $y$ -intercept of  $-269 \text{ eV}$ , indicating that the real laboratory frame collision energy is lower than the potential difference between the source and the surface by 269 eV. The need for this correction in the laboratory collision energy scale can be understood as follows: during the time interval preceding the ion extraction at the source, precursor ions have enough time to fly toward the extraction plate. At the moment of ion extraction, the potential gradient that the ions experience is smaller than the one to which they would be exposed if started exactly at the sample plate. In other words, the displacement in the flight path direction during the extraction delay reduces the distance between the ions and the extraction plate and consequently the electrical field applied to them, thus reducing the effective SID collision energy.

**Surface-Induced Dissociation of MALDI-Generated Peptide Ions.** Figure 7 shows energy-resolved SID spectra of angiotensin III. Figure 7a shows the results for the “parent ion turning” experiment. Panels b and c of Figure 7 show SID spectra at surface dc voltage bias values resulting in laboratory collision energies of 50 and 60 eV respectively. Notice the decrease in parent ion signal and corresponding increase of the ion ratio (immonium ion:  $a_2$  or  $a_2 - \text{NH}_3$ ) when the collision energy is increased from 50 to 60 eV, providing evidence of the correct functioning of the modifications introduced in the spectrometer to perform surface-induced ion activation.

A MALDI TOF SID spectrum of YGGFLR at 50 eV is shown in Figure 8a. In the low-mass end of the MALDI SID spectrum, fragment ion peaks show a fwhm of  $\sim 3 \text{ Da}$  (2.5 Da at  $m/z = 136 \text{ Da}$ ). This spectrum can be compared with the YGGFLR spectrum (at 50 eV collision energy) shown in Figure 8b obtained with the FAB EB/TOF SID instrument reported earlier by our group.<sup>36</sup> The EB/TOF SID spectrum shows fwhm values of 1.5 Da at  $m/z = 136$ . This difference in resolution is attributed mainly to the differences in flight path (525 mm in the MALDI TOF SID instrument vs 775 mm in the FAB EB/TOF SID instrument) and the extraction field that determines the time available for fragmentation prior to analysis. Although both spectra show intense signals in the low-mass end, the spectrum obtained in the FAB

(52) Franzen, J. *Int. J. Mass Spectrom. Ion Processes* **1997**, *164*, 19–34.

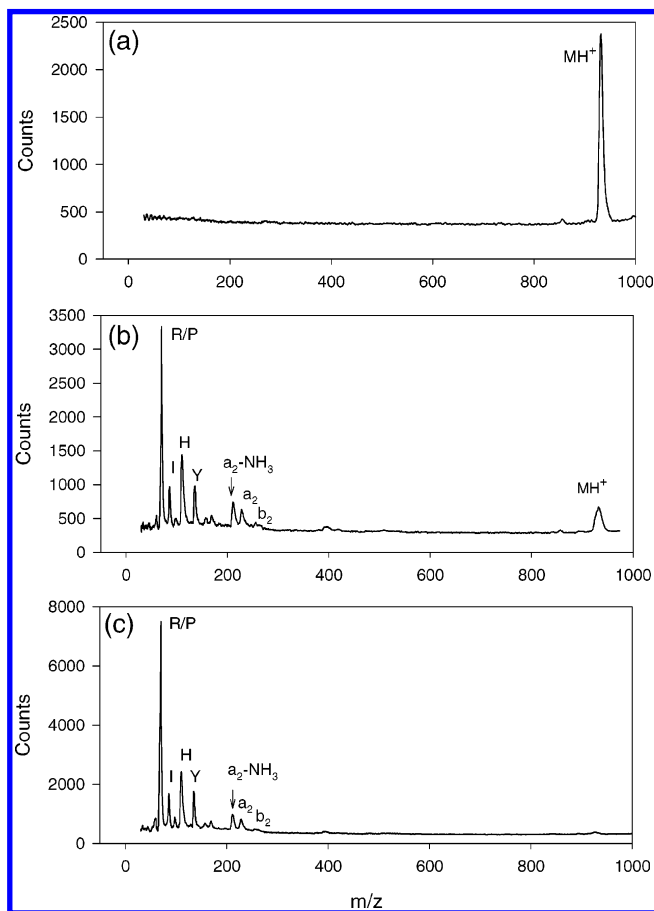


Figure 7. SID spectra for angiotensin III (RVYIHPF): (a) parent ion turning (no collision), (b) 50- and (c) 60-eV collision energies. A total of 300 laser shots were collected in each case. Sample plate, 16.198 kV; extraction plate, 14.900 kV; lenses at the source, 9.791 kV; last reflectron plate, 5.000 kV; surface grid, 12.000 kV; delay of the surface voltage pulse, 12.6  $\mu$ s; extraction delay at the source, 235 ns.

EB/TOF SID instrument shows a larger relative intensity of the F,  $y_1$ ,  $b_2$ , and  $b_3$  ions. While this difference might be partially attributed to differences in internal energy deposited during the ionization step, fragmentation kinetics likely play a role in the differences in relative abundances observed: the  $\text{TOF}_{\text{surface-detector}}$  for protonated YGGFLR is 8  $\mu$ s in the MALDI TOF SID instrument and 27  $\mu$ s in the FAB EB/TOF SID instrument with 0.4 and 2.0  $\mu$ s being the residence times in the corresponding surface extraction regions, respectively. In the short time frame sampled in our benchtop MALDI instrument, only fast-decay products are observed and a larger fraction of the parent ion survives at the same collision energy.<sup>53</sup> The different ratios of L to R and F to Y in the spectra from the two instruments are consistent with this observation time frame. It has been reported in the literature that slower dissociation products can be observed in other SID setups such as those that use trapping instruments<sup>54</sup> or when the SID ions are not immediately pulsed into the TOF analyzer after the collision.<sup>37,38</sup>

#### Investigation of the Time Frame of the Observed Fragmentation Processes. SIMION 7.0 simulations of the trajectories

(53) Laskin, J.; Futrell, J. H. *Mass Spectrom. Rev.* **2003**, *22*, 158–181.

(54) Laskin, J.; Denisov, E. V.; Shukla, A. K.; Barlow, S. E.; Futrell, J. H. *Anal. Chem.* **2002**, *74*, 3255–3261.

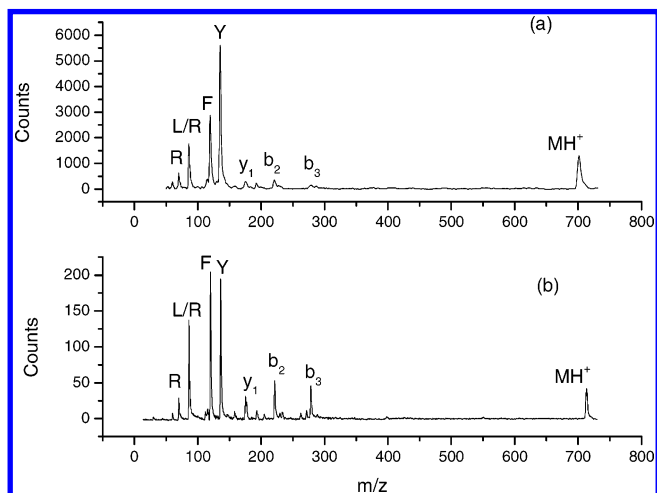


Figure 8. YGGFLR SID spectra obtained at a collision energy of 50 eV using (a) MALDI TOF SID and (b) EB/TOF SID with FAB ionization.<sup>36</sup> A total of 500 shots were collected for the MALDI experiment (1.5-kV extraction pulse, 525-mm flight path). The acquisition time in the EB/TOF experiment was 512 s, equivalent to 2 058 000 gate pulses, each one 800 ns wide (500-V extraction pulse, 775-mm flight path).

of the precursor ion and the fragments were used to model and determine the fragmentation time frame for selected peptide ions. Figure 9a illustrates the major steps of the simulations. In these simulations, the precursor ions were started at the surface with a kinetic energy not exceeding 10 eV for a 50-eV collision to simulate an inelastic scattering event.<sup>55</sup> Their mass was then changed at a specific time (called fragmentation time for simplicity) as shown in Figure 9a. This event simulates the fragmentation process, where at the instant of dissociation the precursor ion's velocity is conserved but the ion's mass decreases so that the kinetic energy is decreased in proportion to the mass. Then, in subsequent calculation steps, the ion's velocity is adjusted according to the electric fields present. The surface voltage pulse was delayed by 740 ns (for a 50-eV collision of protonated YGGFLR) from the precursor ion start time consistent with experimental DSE delay time (Figure 4). All the other electric fields were set to the values used experimentally for a 50-eV collision. The experimental 50-eV collision SID spectrum for YGGFLR is shown in Figure 8a. Figure 9b shows the simulated  $\text{TOF}_{\text{surface-detector}}$  for the protonated YGGFLR fragments as a function of their fragmentation time. As shown in Figure 9b, the  $\text{TOF}_{\text{surface-detector}}$  of the precursor ion (solid line, top) does not change because this ion does not undergo fragmentation. It is evident from Figure 9b that the  $\text{TOF}_{\text{surface-detector}}$  of any fragment ion depends on the time at which the precursor fragments. It is also evident that all  $\text{TOF}_{\text{surface-detector}}$  values for the fragments become closer to that of the intact precursor after a time window of  $\sim 2$   $\mu$ s. After this time window, the fragment formation takes place in the field-free region of the instrument. In this situation, the fragments retain the velocity of the precursor ion, which remains unchanged due to the absence of electrostatic fields, and the fragment ions reach the detector at the same  $\text{TOF}_{\text{surface-detector}}$  as the precursor ions. For YGGFLR, the selected extraction fields and the spacing between electrodes in this

(55) Burroughs, J. A.; Wainhaus, S. B.; Hanley, L. J. *J. Phys. Chem.* **1994**, *98*, 10913–10919.

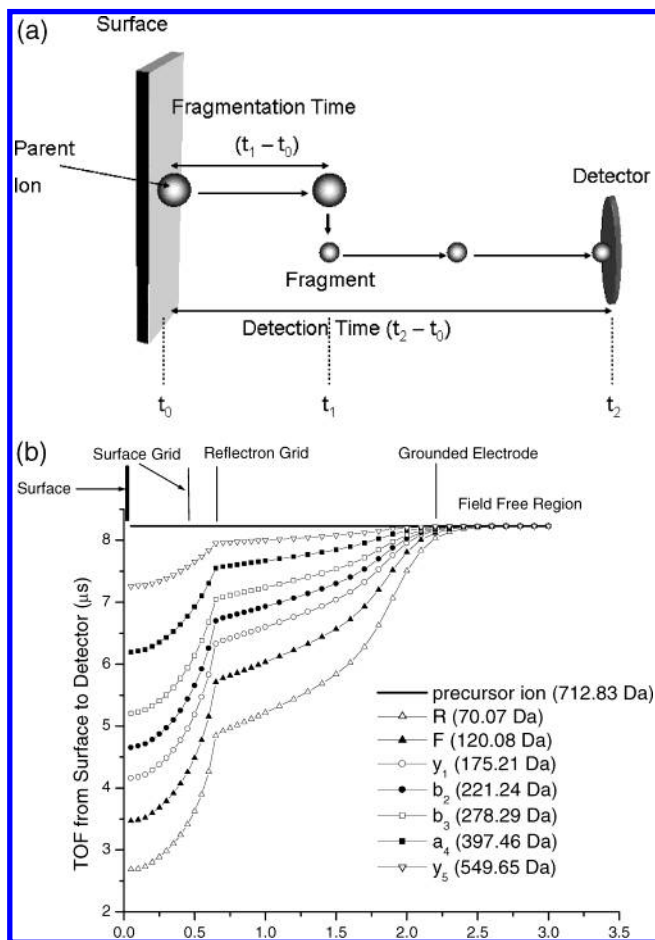


Figure 9. (a) Illustration of the simulated fragmentation time and the simulated detection time calculated with SIMION 3D 7.0. At time ( $t_1 - t_0$ ),  $m/z$  corresponding to activated precursor ion is changed to the  $m/z$  corresponding to a fragment ion. The symbols in (b) correspond to different simulated ( $t_2 - t_0$ ) values ( $y$  axis) and ( $t_1 - t_0$ ) values ( $x$  axis). (b) Simulated flight times (from surface to detector) for several fragments of protonated YGGFLR as a function of the time that the precursor ion is allowed to survive, without fragmenting, after the surface impact. Simulated electric fields are the same as those employed in the 50-eV collision experiment. The relative positions of the surface, grids, and the field-free region with respect to the location of the precursor ion when it fragments are also indicated at the top of the plot.

instrument limit the time window available for fragmentation prior to the arrival at the field-free region to  $\sim 2 \mu\text{s}$ . For the heavier peptide LMYPTYLK, this time window extends to  $2.5 \mu\text{s}$ . These time frames are shorter than those of our FAB EB/TOF SID instrument ( $\sim 20 \mu\text{s}$ ). To match the experimental  $\text{TOF}_{\text{surface-detector}}$  with the simulated  $\text{TOF}_{\text{surface-detector}}$  shown in Figure 9b, the fragment ions observed must have been produced at a fragmentation time between 250 and 300 ns after the surface impact event. The simulated fragment formation times that correspond to the experimental  $\text{TOF}_{\text{surface-detector}}$  values for different YGGFLR fragments are summarized in Table 1. In terms of spatial coordinates, these fragmentation times correspond to fragments produced in proximity to the surface (2.5 mm). We obtained the same general time frame of fragmentation for fragments obtained by SID of the peptides angiotensin III (RVYIHPF, 932 Da), LMYPTYLK (1029 Da), des-R<sup>1</sup>-bradykinin (PPGFSPFR, 905 Da), and des-R<sup>9</sup>-bradykinin (RPPGFSPF, 905 Da) (data not shown). Necessarily, the

Table 1. Simulated Fragment Formation Times Corresponding to the Experimental Surface-to-Detector Flight Times Obtained from the MALDI TOF SID Spectrum of Protonated YGGFLR at 50 eV Collision

mass (Da)	simulated fragmentation time (ns)
70 (R)	330
120 (F)	295
175 ( $y_1$ )	279
221 ( $b_2$ )	262
278 ( $b_3$ )	260

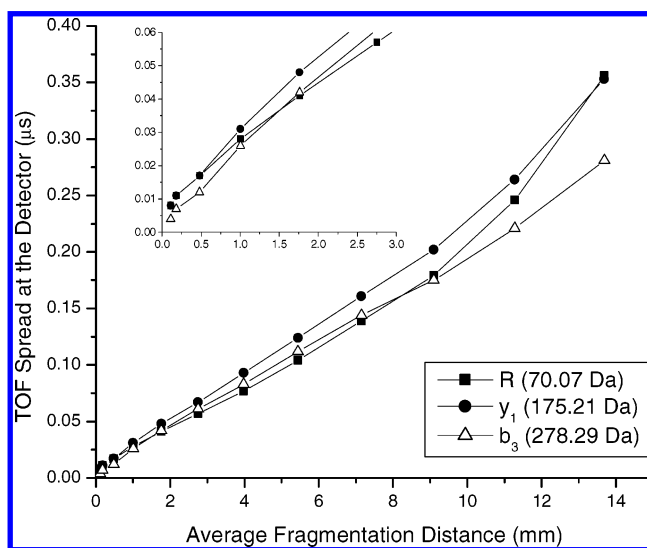


Figure 10. Simulated TOF time spreads at the detector for three fragments of the protonated YGGFLR as a function of the average position of the precursor ion with respect to the surface when it undergoes fragmentation. Simulated electric fields are the same as those employed in the 50-eV collision experiment. The inset shows an expanded region of 0–3 mm from the surface.

specific electrostatic fields used in our experiments are such that they focus the fragment ions formed in the surface-to-grid region, producing peaks in the mass spectrum with an acceptable width (fwhm 20–50 ns). Figure 10 is a plot of simulated  $\text{TOF}_{\text{surface-detector}}$  spreads for three fragments ions (R,  $y_1$ ,  $b_3$ ) as a function of the average fragmentation position from the surface. The simulation results shown in Figure 10 were obtained using an initial TOF spread of 71 ns for the precursor ion packet starting at the surface. This value was determined by a preliminary simulation where ions were flown from the source to the surface with starting conditions in agreement with possible initial energy spreads before acceleration (0–5 eV) and a laser pulse width of 3 ns. According to Figure 10, a simulated  $\text{TOF}_{\text{surface-detector}}$  spread of 20–50 ns for the extraction fields used to obtain the spectrum of Figure 8a corresponds to average fragmentation positions of 1–3 mm away from the surface and a fragmentation time frame of 250–300 ns in agreement with the experimental results and the previous simulation results. Assuming that the ion optics are capable of collecting ions produced at all the different scattering angles and kinetic energies, Figure 10 also illustrates that only the fragment ion signals produced from the decay processes in the time interval from the surface impact event to hundreds of nanoseconds have time widths that result in detectable signal-to-noise ratios. In this

case, this defines the observation time window of this instrument for the studied peptides under the applied extraction conditions.

The possible sources of errors that may contribute to the average TOF<sub>surface-detector</sub> simulation discussed above include the estimation of the delay of the surface extraction (DSE), the estimation of the initial conditions of the precursor ions during the inelastic scattering event from the surface such as the initial kinetic energy, position on the surface, and scattering angle, and errors resulting from errors in distance and voltage measurements. The experimental DSE could be different from the estimated value of 740 ns for YGGFLR. Simulations were performed to estimate the maximum possible error in the predicted fragmentation time frames using extreme values for DSE (in the range of 0–1000 ns). These indicated a maximum possible error of ~50 ns. Another source of error is the estimated starting kinetic energies for the precursor ions that are around or less than 10 eV for a 50-eV collision based on the results reported by Hanley and co-workers.<sup>55</sup> We performed simulations using a range of initial kinetic energies (0–10 eV for a 50-eV collision) obtaining the same time frame for the formation of the observed fragment ions (250–300 ns). This result indicates that the kinetic energy of the surface-scattered ions does not have a significant effect on the final arrival time distribution of the fragment ions at the detector because kinetic energies achieved by the extraction fields are more than 2 orders of magnitude greater than this initial scattering energy. According to our simulations, the different initial positions (modeled for random positions in a 10 mm × 10 mm square region at the surface center) and scattering angles for the precursor ion beam at the surface (modeled for scattering angles in the range of 0–90°) may contribute to the maximum possible error by ~20 ns. To evaluate the contribution to the error arising from distance measurements used for SIMION drawings of the commercial part of the instrument, experimental source-to-detector TOF of a known analyte was compared to the simulated value. For example, in the regular reflectron mode, the experimental and simulated source to detector TOF values for protonated YGGFLR are 20.918 and 20.911 μs, respectively, with only a 7-ns difference. The other distance measurements in the introduced surface assembly region are performed with a digital caliper (model CD-S6"CT, Mitutoyo Corp.), which introduces errors of ±0.02 mm. As mentioned in the Experimental Section, the voltage measurements were performed using the monitor outputs of the power supplies with a precision of 5 V. Therefore, considering all the possible sources of errors, we estimate a maximum possible systematic error of less than +100 ns in the estimation of the formation times of the fragments. Even with this maximum possible error, our estimated 250–300-ns time frame of formation for the major fragment ions in the spectrum shown in Figure 8a falls in the 100-ns range.

As an additional method of validating the fragmentation times that we report here, a similar comparison between experimental arrival times and SIMION simulations was performed for the 50-eV FAB EB/TOF SID spectrum of YGGFLR (Figure 8b). As mentioned earlier, the EB/TOF SID instrument has a much lower surface extraction field (500 vs 7200 V/cm for MALDI TOF), resulting in longer times spent in the extraction region for the SID ions (2-μs FAB EB TOF SID vs 0.4-μs MALDI TOF SID). We obtained fragmentation times in the range of 250–300 ns (~1

Table 2. Simulated Fragment Formation Times Corresponding to the Experimental Surface-to-Detector Flight Times Obtained from the MALDI TOF SID Spectra of Protonated LMYPTYLK at Two Different Collision Energies

mass (Da)	fragmentation time (ns)	
	40 eV	60 eV
70 (P)	292	276
104 (M)	265	247
136 (Y)	245	228
217 (a <sub>2</sub> )	211	193
245 (b <sub>2</sub> )	204	167
277 (YL)	119	89

mm away from the surface) for this instrument, consistent with the MALDI TOF SID results.

We have also conducted experiments followed by SIMION simulations to investigate the energy dependency of the fragmentation time frame. Table 2 summarizes the results for the observed MALDI TOF SID fragments of protonated LMYPTYLK at two different collision energies, 40 and 60 eV. It is evident that, at a collision energy of 60 eV, the obtained fragmentation times are consistently shorter than those at 40 eV, which is in agreement with the higher internal energy deposition at higher collision energies leading to larger rate constants for the decay process. Note that we have obtained a fragmentation time as small as 89 ns for the internal fragment YL for a 60-eV collision. A discussion of the relative differences in fragmentation time frames for each type of fragment is beyond the scope of this paper and awaits further experimental and conceptual developments. However, the fact that different fragmentation pathways have different fragmentation times illustrates that the phenomena observed in our experiments are a function of the precursor ions' molecular structure and associated fragmentation pathways and not an artifact of the measurements or simulations.

The above results indicating fragment formation in proximity to the surface imply a fast-fragmentation process but do not correspond to immediate fragmentation upon surface impact. Laskin et al. have also studied the fragmentation kinetics of peptides upon collision with a surface using an FTICR SID instrument.<sup>41,56</sup> Using time-resolved SID spectra and RRKM modeling of their experimental data, they were able to distinguish between two different decay rates for observed fragments, which they referred to as "slow" and "fast". They described the fast-fragmentation process as the molecule fragmenting after reaching a certain internal energy threshold (~10 eV) on or very near the surface.<sup>56</sup> They referred to this decay process as a "sudden death" or "shattering" process, a term coined by others in describing surface-induced dissociation of atomic clusters.<sup>57</sup> Although these terms convey the concept of the instantaneous nature of the process, the time frame for the suggested "shattering" process for the peptides at hyperthermal collision energies cannot be directly derived from their work, partly because their instrumental setup is not designed to monitor fragmentation times shorter than a few milliseconds. Our combined experimental and simulation studies indicate a decay process occurring close to the surface

(56) Laskin, J.; Futrell, J. H. *J. Am. Soc. Mass Spectrom.* **2003**, *14*, 1340–1347.

(57) Raz, T.; Even, U.; Levine, R. D. *J. Chem. Phys.* **1995**, *103*, 5394–5409.

(2–3 mm) under the extraction conditions used, in a hundreds of nanoseconds time frame. We also performed simulations for a surface-shattering process and obtained no experimental evidence (ion signals) that match the calculated  $\text{TOF}_{\text{surface-detector}}$  under the employed extraction conditions. Energy-resolved studies shown in Table 2 indicate decay processes that depend on the amount of kinetic energy of the impacting precursor ion. The faster rate observed at 60 versus 40 eV collision for protonated LMYPTYLK indicates fast-decay processes that depend on the amount of internal excitation rather than an instantaneous process taking place during the residence time of the ion at the surface. The above results of a submicrosecond time frame decay suggest a rate constant in the range of  $10^6$ – $10^7$   $\text{s}^{-1}$  for the observed fast-fragmentation processes.

## CONCLUSIONS

This study shows the feasibility of surface-induced activation of MALDI-generated peptide ions in a TOF analyzer using a close-to-normal collision geometry. Simulations with SIMION 7.0 indicate a fragmentation time frame in the nanosecond region ( $10^6$ – $10^7$   $\text{s}^{-1}$  rate constant) corresponding to an average fragmentation region located 1–3 mm away from the surface, for the studied peptides and extraction fields used. This instrument will prove useful in further kinetic studies of these submicrosecond fragmentation processes of peptides. Currently, we are conducting experiments to improve the mass resolution and accuracy of the measurements. These include lowering the static extraction fields at the surface as a way to increase the residence times of the ions and improve the effectiveness of the delayed extraction pulse.

(58) Moskovets, E.; Karger, B. L. *Rapid Commun. Mass Spectrom.* **2003**, *17*, 229–237.

(59) Schlosser, A.; Lehmann, W. D. *Proteomics* **2002**, *2*, 524–533.

(60) Fernandez, F. M.; Smith, L. L.; Kuppannan, K.; Yang, X.; Wysocki, V. H. *J. Am. Soc. Mass Spectrom.* **2003**, *14*, 1387–1401.

Improving the delayed ion extraction at the surface by using exponential extraction pulses<sup>52</sup> is another potential future direction. Improvements in the calibration procedure are also possible. Moskovets and Karger have reported increased mass accuracy for MALDI TOF MS with the inclusion of a term in the calibration formula that accounts for the finite rise time of the delayed extraction pulse at the source.<sup>58</sup> This approach could also be applied to the delayed extraction of the SID ions at the surface.

We are also investigating the replacement of the planar collision target holder with a thick (9 mm) cylindrical extraction–collimation electrode to investigate whether improvements in the collection efficiency of the fragment ions produced at or close to the surface are possible. If larger mass fragments are formed in the increased reaction time frame of the instrument, but are lost due to ion collection deficiencies at large scattering angles, new ion optics might prove beneficial. Information from the observed ion signals can be used in an alternative peptide sequencing approach such as the “Patchwork” peptide sequencing method recently described<sup>59</sup> that we have adapted to SID data.<sup>60</sup>

## ACKNOWLEDGMENT

We acknowledge Bruker Daltonics for the donation of a Proflex MALDI TOF MS and Dr. Mel Park and Mr. Doug Roderick for helpful discussions. Material is based upon work supported by the National Science Foundation under Grant DBI-0244437; the DBI instrumentation research provided data for a proposal, now funded, that will allow continuation of the fragmentation kinetics research under Grant CHE-0416388. We thank Dr. Ronald Wysocki for the synthesis of 2-(perfluorodecyl)ethanethiol.

Received for review May 10, 2004. Accepted June 23, 2004.

AC0493121